

New SAR Target Recognition Based on YOLO and Very Deep Multi-Canonical Correlation Analysis

Moussa Amrani*, Abdelatif Bey, and Abdenour Amamra

Ecole Militaire Polytechnique, Chahid Abderrahmane Taleb, Algiers, Algeria

Abstract. Synthetic Aperture Radar (SAR) images are prone to be contaminated by noise, which makes it very difficult to perform target classification in SAR images. Inspired by great success of very deep convolutional neural networks (CNNs), this paper proposes a robust feature extraction method for SAR image target classification by adaptively fusing effective features from different CNN layers. First, YOLOv4 network is fine-tuned to detect the targets from the respective MF SAR target images. Second, a very deep CNN is trained from scratch on the moving and stationary target acquisition and recognition (MSTAR) database by using small filters throughout the whole net to reduce the speckle noise. Besides, using small-size convolution filters decreases the number of parameters in each layer and therefore reduces computation cost as the CNN goes deeper. The resulting CNN model is capable of extracting very deep features from the target images without performing any noise filtering or pre-processing techniques. Third, our approach proposes to use the multi-canonical correlation analysis (MCCA) to adaptively learn CNN features from different layers such that the resulting representations are highly linearly correlated and therefore can achieve better classification accuracy even if a simple linear support vector machine (SVM) is used. Experimental results on the MSTAR dataset demonstrate that the proposed method outperforms the state-of-the-art methods.

Keywords: Synthetic Aperture Radar, YOLO, Target classification, Very deep features, Feature fusion, MCCA.

1 Introduction

SYNTHETIC aperture radar (SAR) is a very high-resolution airborne and space-borne remote sensing system for imaging distant targets on a terrain, which can operate proficiently in all-weather day-and-night conditions and generate images of extremely high resolution. A SAR system sends electromagnetic pulses from radar mounted on a moving platform to a fixed particular area of interest on the target and combines the returned signals coherently to achieve a very high-resolution depiction of the scene.

SAR has been substantially employed for many applications such as surveillance, reconnaissance, and classification. However, speckle greatly disrupts SAR image readability, which makes defining discriminative and descriptive features a hard task. To address this problem, several feature processing methods have been advanced and utilized to understand the target from SAR images such as geometric descriptors, and transform-domain coefficients [1]. Although the above-mentioned methods may have some advantages, most of these methods are hand-designed and relatively simple [2]. Besides, they failed to achieve the promising classification performance (i.e., accuracy) [3]. Recently, deep convolutional neural networks (DCNNs) have been referenced by several authors to design classification algorithms for SAR images [4,5]. A deep neural network is an artificial network with multiple hidden layers between the input and the output. In [4] the

authors proposed A-ConvNets which consists of sparsely connected layers to reduce the number of free parameters from over-fitting. After implementing data augmentation, the network is trained using mini-batch stochastic gradient descent with momentum and back-propagation algorithm. Then, a soft-max layer is applied to output a probability distribution over class labels. One of the uncertain points of this method is that the convolutional layers suffer less from over-fitting because they have smaller number of parameters compared to the number of activations. Therefore, adding dropout to convolutional layers slows down the training [5]. In addition, they employed cropped patches of 88×88 from the original SAR images in the training phase (i.e., as data augmentation) to deal with the translation invariance of DCNN for SAR-ATR system [6]. The other well-known deep learning based algorithm [7] focuses on solving the classification problem by learning randomly sampled image patches using unsupervised sparse auto-encoder instead of using the classical back-propagation algorithm. Then a single layer of convolutional neural network is used to automatically learn features from SAR images. These feature maps are then adopted to train the final soft-max classifier, which results in a little low classification accuracy [8]. The research in [9], proposes to select deep features for SAR target classification task, in which the top layers of CNNs contain more semantic information and describe the global features of the images, whereas the intermediate layers describe the local features, and the bottom layers contain more low-level information for the description of texture, edges, etc. However, the authors used large kernels in the first and the second layers, which increase the number of parameters and have less discriminative decision functions. Moreover, they adopted a pre-processing method to remove some noise from target images, and metric learning for feature selection to adjust the accuracy level, which is time consuming.

More recently, very deep CNNs using small-size convolution filters have been used by Ciresan et al [10]. However, their networks are significantly less deep and they have not been evaluated on SAR images. Goodfellow et al. [11] applied very deep ConvNets (11 weight layers) to street number recognition tasks and have depicted that increasing the depth of the network produces better performance. Szegedy et al. [12], an ILSVRC-2014 top-performing classification task, has developed independently a network based on very deep ConvNets (22 weight layers) and small convolution filters. However, their network is more complex and the spatial resolution of the feature maps in the first layers is sharply reduced to decrease the computation amount [13]. C.P. Schwegmann et al. [14] have introduced very deep features for ship discrimination in SAR images.

When trained on a small database, their proposed very deep high network can provide better classification performance than conventional DCNNs.

Compared to the handcrafted and deep features, our approach uses very deep features to have more powerful discriminative and robust representation abilities, and multi-canonical correlation analysis (MCCA) algorithm to maximize the correlation among the feature sets, remove irrelevant features and overcome the curse of dimensionality issue. The contributions of the proposal method mainly include two aspects.

- YOLOv4 is used for SAR target detection. Besides, a very deep network is proposed for SAR image target classification, which uses very small receptive small filter sizes throughout the whole net to reduce the speckle noise that degrades the quality of SAR images, and therefore achieves better performance as we go deeper.
- Multi-Canonical Correlation Analysis (MCCA) is proposed to adaptively select and fuse CNN features from different layers and such that the resulting representations are highly linearly correlated and therefore remove irrelevant features, speed up the training task, and improve the classification accuracy. As a result, we come up with **particularly** more accurate CNN-SAR architecture, which achieves the state-of-the-art accuracy on **MSATR SAR target** recognition tasks.

even when adopted as a relatively simple pipeline.

The rest of this paper is organized as follows. Section 2 describes the framework of the proposed method and introduces the feature fusion method using MCCA. The experimental results are presented in Section 3. Finally, Section 4 gives the concluding remarks of the paper.

2 YOLOv4 Target detection

YOLOv4 combines many advanced target detection techniques to improve the accuracy and running speed of CNN as it is clarified in Figure 1. It can be run in real-time on a typical GPU, which makes it widely used. Yolo V4 consists of four parts. The main methods and tricks utilized in each part are as follows [15]: **Input:** Mosaic data augmentation, cross mini batch normalization (CmBN), and self-adversarial training (SAT). **BackBone:** Cross stage partial connections Darknet53 (CSPDarknet53), mish-activation, and dropblock regularization. **Neck:** SPP, modified feature pyramid network (FPN), path aggregation network (PAN). Prediction: Modified complete IOU (C-IOU) loss, distance IOU (D-IOU) nms. Some of these tricks can

obviously improve the network performance. Mosaic data augmentation mixes four training images with clipping and scaling, which significantly reduces the requirement for large mini-batch processing and GPU computing. SAT alters the original SAR image to create the deception of undesired object. These modified images are used for network training in next stage, which could improve the robustness of the network. Cross stage partial connections split the gradient flow propagate into different network paths, which greatly reduces the amount of computation, and improves the inference speed of the network. Other tricks also improve the other details of the networks. For example, SPP, FPN and PAN improve the feature extraction. Modified C-IOU loss and DIOU nms improve the IOU loss to achieve better convergence speed and accuracy of regression problem.

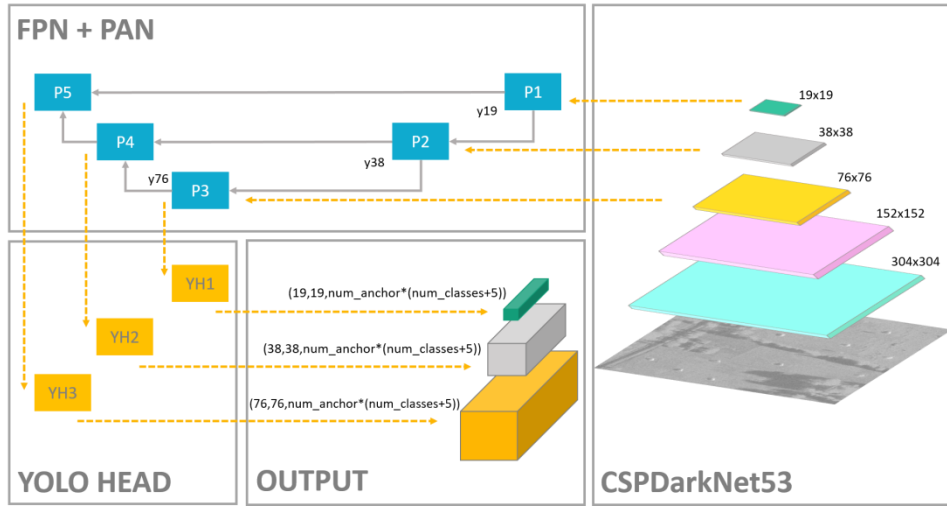


Fig.1. The architecture of YOLOv4

3 The Proposed Method for SAR Target Recognition

Inspired by great success of very deep convolutional neural networks (VDCNNs), this paper presents a robust feature extraction method for SAR target classification using very deep features without performing any noise filtering or pre-processing techniques. Figure 2 shows the main steps of the proposed network: after targets detection from the respective SAR target images, SAR Oriented Network (SARON) is used for extracting very deep features from detected data. Then the resulting deep features are then selected and fused by MCCA. Finally, the classification of the

targets with respect to its training set is done according to the classification error rates using SVM.

In the following sections, each step of the proposed method is described in detail.

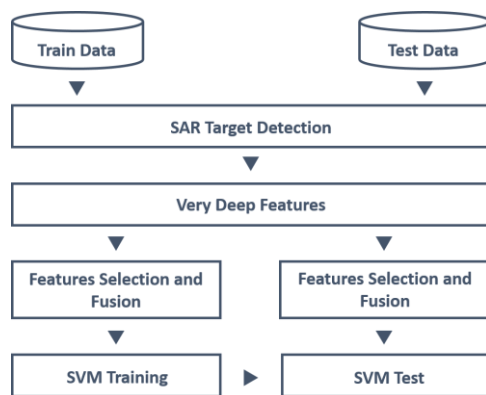


Fig.2. Overall architecture of the proposed method

3.1 SAR Oriented Network

Using deep neural networks to learn effective feature representations has become popular in SAR target classification [4, 5, 16, 17]. It is also employed in the military field as automatic target recognition (ATR) [18]. In contrast to most DCNNs that usually have five or seven layers, the proposed network is based on the very deep VGG net for feature extraction, which has a much deeper architecture (up to 19 weight layers) and hence can provide much informative and descriptive features [13]. To achieve better classification performance, the network is fine-tuned from scratch on the MSTAR database and then the fine-tuned network is treated as a fixed feature descriptor for SAR target images.

Figure 3 shows the architecture of the proposed very deep CNN model, which is a stack of convolutional layers (Conv.) followed by three fully-connected (Fc.) layers, and each stack of Conv. is followed by a max pooling layer (Pool.). Besides, all hidden layers are supplied with ReLU. Fc.1 is regularized using dropout technique, while the last layer acts as a C-class SVM classifier. Figure 4 shows the outputs from the first convolutional layer corresponding to a sample SAR image from the MSTAR dataset.

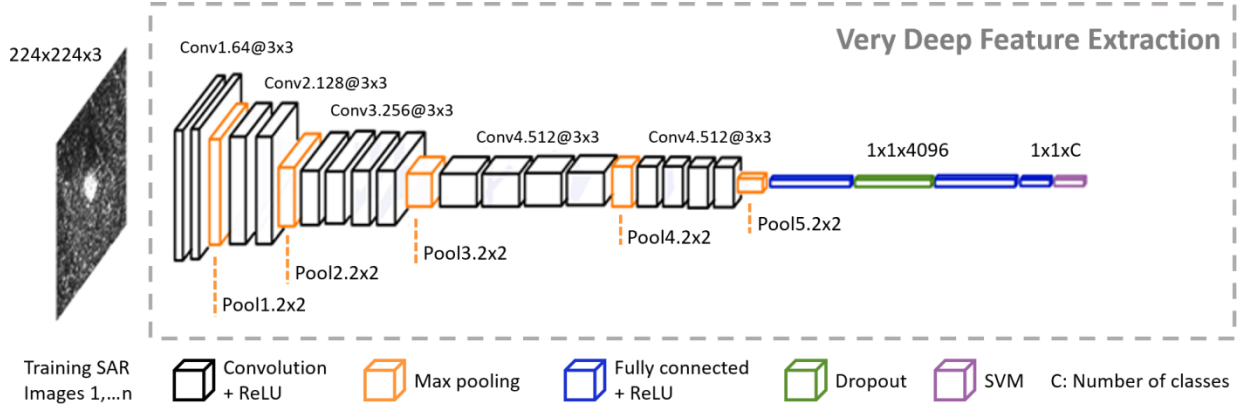


Fig.3.The proposed SAR oriented very deep network for target image classification

3.1.1 Configuration

The network used in this paper has 19 weight layers (16 conv. and 3 Fc. layers). The width of the convolutional layers (channels number) is quite small, which begins from 64 in the first layer, then increases by a factor of 2 after each max pooling layer until it reaches 512.

Our Network configuration is rather different from the ones used in the previous MSTAR SAR target classification [4, 9, 15, 17]. Rather than using relatively large receptive fields in the first conv. layers (e.g. 13×13 with stride 4 in [15]), 7×7 with stride 1 in [9], or 5×5 with stride 1 in [4]), we use very small 3×3 receptive fields throughout the whole net, which are convolved with the input at every pixel (with stride 1). Furthermore, we remove local response normalization (LRN) as it does not improve the performance on our SAR images dataset but leading to increase the computation time and the memory consumption, and we modify the output layers to appropriately match the C classes in our data set. The configuration of the fully connected layers is the same in all network and all hidden layers are supplied with the rectified linear unit (ReLU) to have more discriminative decision functions and lower computation cost [13, 19]. To achieve better classification accuracy, the linear support vector machine ($L2$ -SVM) is used as a baseline classifier instead of maximum entropy classifier [18, 20]. Consequently, we come up with expressively more

accurate CNN architecture, which achieves the state-of-the-art accuracy on SAR target classification task.

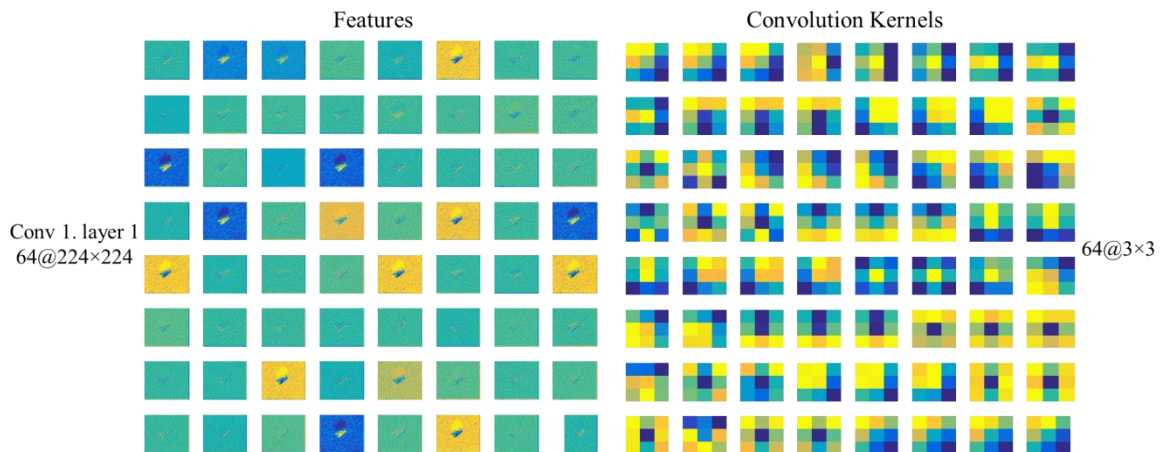


Fig.4. (Left) Output feature maps and (right) Learned kernels of the first layer.

3.2 MCCA Based Feature level Fusion

Our proposed method is based on the fusion of the very deep features learned by our network model. The outputs of some selected layers are used as a feature descriptor of the input target. In particular, we considered the fully connected layers output with 4096 feature channels, which contain more low-level information for the description of texture and edges.

Several feature fusion methods have been proposed to obtain more informative descriptors to describe the image targets. The serial strategy [21] simply combines two feature sets into one real union-vector and assumes that x and y are two feature sets with p and q vector dimensions, respectively. Contrary to the serial feature fusion, the parallel strategy [22] combines the two feature sets into a complex feature set $z = x + iy$ where i is the imaginary unit. However, these strategies neglect the class structure among the sample images and attain high dimension of the fused feature sets. Besides, SAR images have their own characteristics (speckle noise, illumination, pose variations, depression angle, corruption, and occlusion), and the choice of features is dictated by the statistical structure of the data [23].

Let $X_{(p \times n)}$ and $Y_{(q \times n)}$ be two matrices that contain n training feature vectors. In our study, we adopt CCA [24, 25] to find the linear combination a^T and b^T that maximize the pairwise correlations $X^* = a^T X$ and $Y^* = b^T Y$ across the two feature sets, restrict the correlations to be between classes, and to face noise [26]. The top layers of our proposed SAR-OVDN contain more semantic

information and describe the global feature of the images, whereas the intermediate layers describe the local features, and the bottom layers contain more low-level information for the description of texture, edges. MCCA is proposed to combine information from different levels to obtain distinguishing (relevant) features and overcome the curse of dimensionality problem. The transformation matrices a and b are diagonalized by solving the eigenvalue equations as [27]:

$$V = \begin{pmatrix} \text{cov}(x) & \text{cov}(x, y) \\ \text{cov}(y, x) & \text{cov}(y) \end{pmatrix} = \begin{pmatrix} V_{xx} & V_{xy} \\ V_{yx} & V_{yy} \end{pmatrix} \quad (4)$$

$$\begin{cases} V_{xx}^{-1}V_{xy}V_{yy}^{-1}V_{yx}\hat{a} = \Lambda^2\hat{a} \\ V_{yy}^{-1}V_{yx}V_{xx}^{-1}V_{xy}\hat{b} = \Lambda^2\hat{b} \end{cases} \quad (5)$$

where \hat{a} and \hat{b} are the eigenvectors and Λ^2 is the eigenvalues diagonal matrix, the non-zero eigenvalues number in each equation is $r = \text{rank}(V_{xy}) \leq \min(n, p, q)$ that is organized in decreasing order, $\gamma_1 \geq \gamma_2 \geq \dots \geq \gamma_r$, the transformation matrices a and b contain the consistent eigenvectors to the non-zero eigenvalues, and $X^*, Y^* \in \mathfrak{R}^{r \times n}$ are the canonical variates. To find the transformed training features sets, the covariance matrix in Equation 4 will be defined as:

$$V^* = \left(\begin{array}{cccc|cccc} 1 & 0 & \cdots & 0 & \gamma_1 & 0 & \cdots & 0 \\ 0 & 1 & \cdots & 0 & 0 & \gamma_2 & \cdots & 0 \\ \vdots & & \ddots & & \vdots & & \ddots & \\ 0 & 0 & \cdots & 1 & 0 & 0 & \cdots & \gamma_r \\ \gamma_1 & 0 & \cdots & 0 & 1 & 0 & \cdots & 0 \\ 0 & \gamma_2 & \cdots & 0 & 0 & 1 & \cdots & 0 \\ \vdots & & \ddots & & \vdots & & \ddots & \\ 0 & 0 & \cdots & \gamma_r & 0 & 0 & \cdots & 1 \end{array} \right) \quad (6)$$

where the canonical variates have nonzero correlation only on their relative indices. The upper left and lower right corners in the identity matrices indicate that the canonical variates are uncorrelated with in training features sets. Figure 5 shows the statistical transformation of the CCA framework.

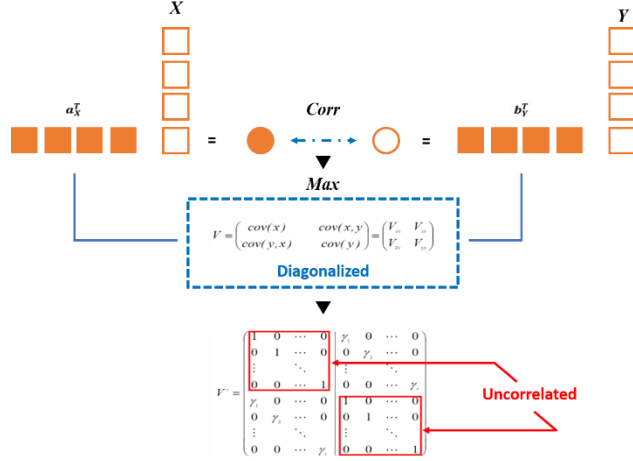


Fig.5. CCA transformation framework

In our work, feature-level fusion is then performed by using summation of the transformed feature vectors as:

$$M = X^* + Y^* = a^T X + b^T Y = \begin{pmatrix} a \\ b \end{pmatrix}^T \begin{pmatrix} X \\ Y \end{pmatrix} \quad (7)$$

where M is the Very Deep Canonical Correlation Discriminant Features (VDCCDFs). Multi-canonical correlation analysis (MCCA) generalizes CCA to be appropriate for more than two features sets. We suppose that we have λ feature sets $F_i \in \mathbb{R}^{p_i \times n}$, $i = 1, 2, \dots, \lambda$, which are arranged based on their rank, $\text{rank}(F_1) \geq \text{rank}(F_2) \geq \dots \geq \text{rank}(F_k)$. MCCA applies CCA to two features sets at the same time. In each phase, the two feature sets with the highest ranks are fused together to keep the maximum possible feature vectors length as shown in Figure 6.

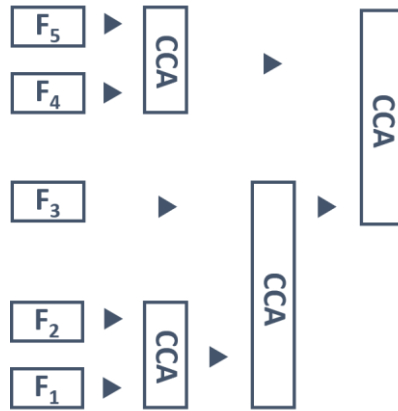


Fig.6. Multi-canonical correlation analysis techniques for five sample sets with $\text{rank}(F_1) > \text{rank}(F_2) > \text{rank}(F_3) > \text{rank}(F_4) = \text{rank}(F_5)$

3.3 Support Vector Machine (L2-SVM)

Recently, most of the deep learning models utilize multi-class logistic regression for prediction and minimize cross-entropy loss for SAR target classification [4, 5, 16, 28]. In this paper, for better performance and parameter optimization, L2-SVM [20] is adopted to train our SAR Oriented Very deep CNN model, when the learning minimizes a margin-based loss by back propagating the gradients from the top layer linear SVM. Therefore, we differentiate the SVM objective function with respect to the activation of the penultimate layer as follows. Let $x_n \in \mathfrak{R}^D$ be training feature set and y_n its labels, where $n=1, \dots, N$, and $t_n \in \{-1, +1\}$. Given the objective $L(w)$ in Equation 8, and the input x is replaced with the penultimate activation m as:

$$\min_w \frac{1}{2} w^T w + C \sum_{n=1}^N \max(1 - w^T x_n t_n, 0) \quad (8)$$

$$\frac{\partial L(w)}{\partial m_n} = -C t_n w (II\{1 > w^T m_n t_n\}) \quad (9)$$

where $II\{\cdot\}$ is the indicator function and C is a constant ($C \geq 0$). As before, for the L2-SVM, we have:

$$\frac{\partial l(w)}{\partial m_n} = -2C t_n w (\max(1 - w^T m_n t_n, 0)) \quad (10)$$

Based on this point, the back-propagation algorithm is just the same as the standard soft-max for deep learning networks.

4 Experimental Results and Analysis

The results of SAR target detection based on the MF dataset, and to validate the effectiveness of the proposed method we conduct extensive experiments on two MSTAR datasets, which are publically available [29]. In the following sections, we first describe the implementation details, and then introduce the used datasets. Finally, the experimental results are presented and analyzed.

4.1 Implementation details

The pre-trained AlexNet, CaffeRef, VGGs and Very Deep-16 are fine-tuned on real SAR images from MSTAR database. The proposed network SARON is trained on a 2.7-GHz CPU with 64 GB of memory and a moderate graphics processing unit (GPU) card. All methods have been

implemented using Microsoft Windows 10 Pro 64-bit and MATLAB R2016a. We randomly select the SAR image samples for the training and the testing datasets.

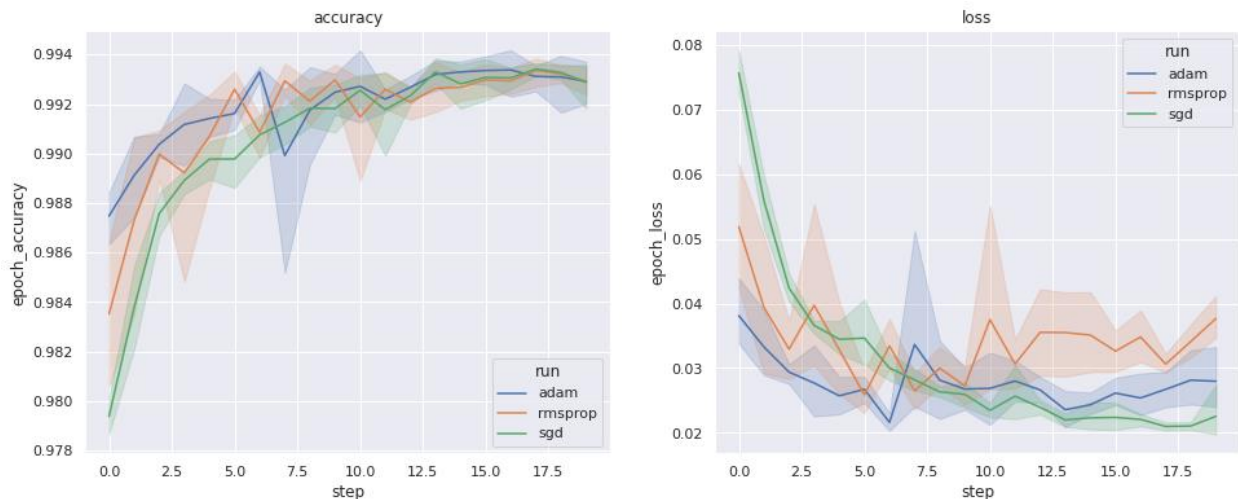


Fig.7. The effect of optimization methods on the performance.

To study the effect of adaptive optimization algorithms on the accuracy in SAR image recognition system, several successful methods such as Stochastic Gradient Descent (sgd), Adam, RMSPROP are evaluated in our work as it is depicted in Figure 7, where the training is carried out by optimizing the primal L2-SVM objective to learn lower level features, the batch size is set to 64, a momentum parameter to 0.9. The training is regularized by weight decay (L_2 penalty multiplier set to 5×10^{-4}) and dropout regularization for the first fully-connected layer (dropout ratio set to 0.5). The learning rate is initially set to 10^{-2} , and then is decreased by a factor of 10 when the accuracy of the validation set stopped improving. In total, the learning rate was decreased 2 times, and the learning has been stopped after 73 epochs. The classification of the targets with respect to its training set is done according to the classification error rates using the linear SVM. The main advantages of our proposed method as follows: first, using small-size convolution throughout the whole net to reduce the speckle noise. Second, decreases the number of parameters in each layer and therefore reduces computation cost as the CNN goes deeper. Moreover, ReLU layers are integrated to have more discriminative decision functions and lower computation cost. Third, the MCCA algorithm is utilized to fuse the feature vectors from the fully connected layers by summation and concatenation forming new robust and discriminant features. The analysis of the advantages is discussed in the following subsections.

4.2 Datasets

The SAR images used in experiments are from the Moving and Stationary Target Acquisition and Recognition (MSTAR) database. This benchmark data is acquired by the Sandia National Laboratories Twin Otter SAR sensor payload, operating at X-band with a high resolution of 0.3 m, spotlight mode, and HH single 320 polarizations (i.e., single-channel): where the phase content is entirely discarded because it is random and uniformly distributed [30, 31]. The first dataset is the MSTAR public mixed target dataset which includes ten military vehicle targets: (armored personnel carrier: BMP-2, BRDM-2, BTR-60, and BTR-70; tank: T-62, T-72; rocket launcher: 2S1; air defense unit: ZSU-234; truck: ZIL-131; bulldozer: D7). The optical images and their relative SAR images are shown in Figure 8.

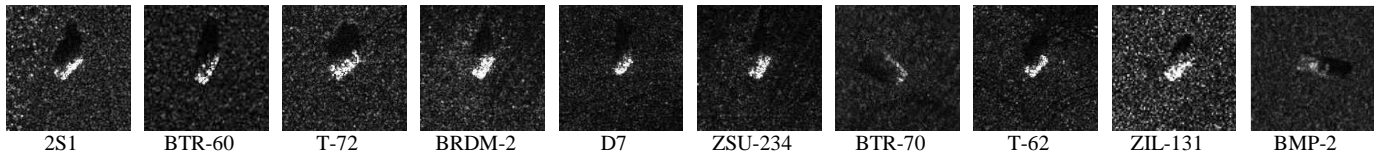


Fig.8. Types of military targets: optical images in the top associated with their relative SAR images in the bottom

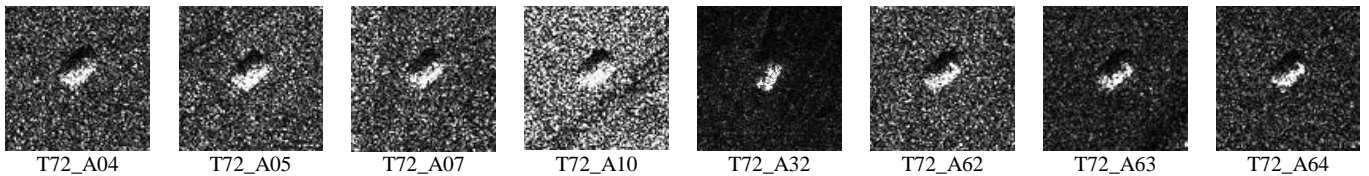


Fig.9. T-72 multi variants: optical images in the top associated with their relative SAR images in the bottom.

The second dataset chosen for evaluation is the MSTAR public T-72 Variants dataset, which contains eight T-72 variants: A04, A05, A07, A10, A32, A62, A63, and A64. Optical images and the corresponding SAR images of the eight T-72 targets are shown in Figure 9.

4.3 Results on the MSTAR Public Mixed Target Dataset

The dataset details including depression angles with target signatures of all MSTAR images used in this task are listed in Table 1. BMP-2 and BTR-70 refers to man-made (metal) objects armored personnel carrier targets, and T-72 refers to main battle tank. The single and overall accuracies are well explained in Tables 2 and 3, respectively. The confusion matrix is clarified in Figure 10.

TABLE 1 MSTAR PUBLIC MIXED TARGET DATASET: THE NUMBER OF TRAINING AND TESTING SAMPLES USED IN THE EXPERIMENTS

Target	Train		Test		
	Depression	Number of Images	Depression	Number of Images	
BMP-2	SN-C21	17°	233	15°	196
	SN-9563	17°	233	15°	195
	SN-9566	17°	232	15°	196
BTR-70	17°	233	15°	196	
T-72	SN-132	17°	232	15°	196
	SN-812	17°	231	15°	195
	SN-S7	17°	228	15°	191
BTR-60	17°	256	15°	196	
2S1	17°	299	15°	274	
BRDM-2	17°	299	15°	274	
D7	17°	299	15°	274	
T-62	17°	299	15°	274	
ZIL-131	17°	299	15°	274	
ZSU-234	17°	299	15°	274	

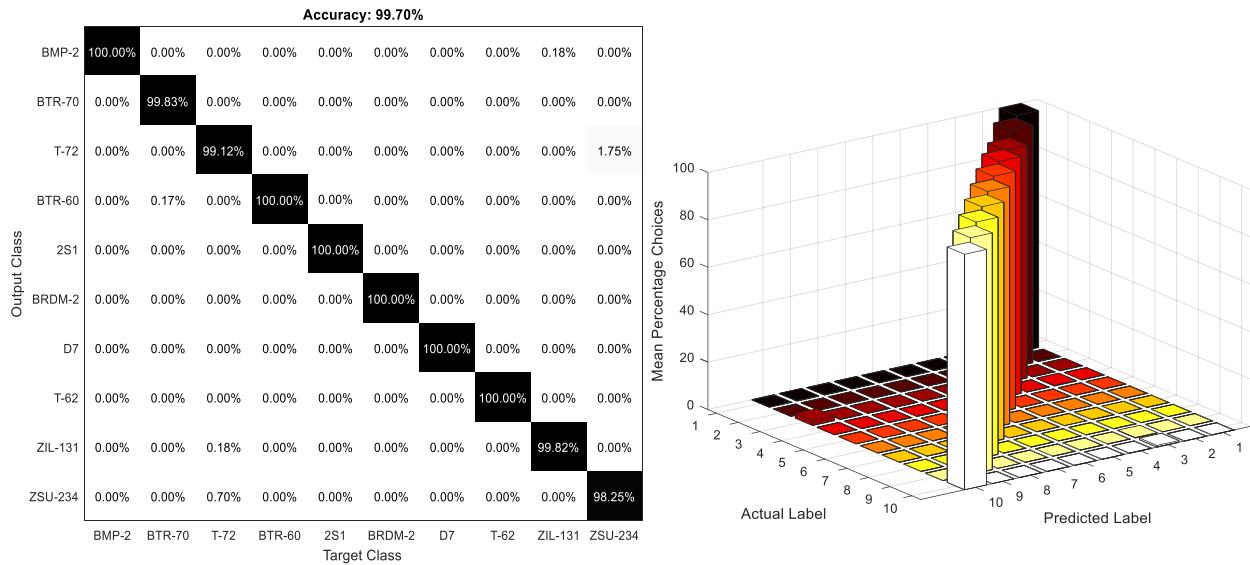


Fig.10. Confusion matrix of the proposed method on MSTAR public mixed target dataset. The rows and columns of the matrix indicate the actual and predicted classes, respectively.

The noise in SAR images can be multiplicative or additive [32, 33]. Figure 11 shows the noise simulation scheme, where the value of a randomly selected pixel is replaced by a value from a uniform distribution. The anti-noise performance of the proposed method is compared with the noise simulation paradigm in [4, 34] and shows that our proposed method is more robust to noise corruption as clarified in Table 4.

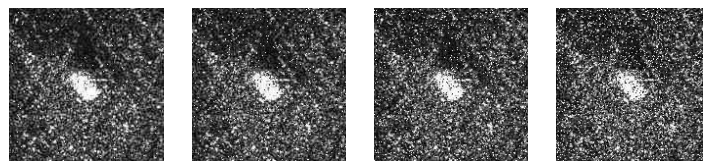


Fig. 11. Illustration of random noise. The levels of noise are 1%, 5%, 10%, and 15%, respectively

TABLE 4 ACCURACIES ACROSS THE LEVEL OF NOISE

Noise	1%	5%	10%	15%
A-Convnets [4]	0.9176	0.8852	0.7584	0.5468
SRC [34]	0.9276	0.8639	0.8049	0.6419
SVM [34]	0.8826	0.8451	0.5310	0.4242
KNN [34]	0.9341	0.8579	0.8177	0.5573
MSRC [34]	0.9488	0.8739	0.8476	0.6853
SAR-Oriented GBVS [35]	0.9216	0.8922	0.7609	0.5578
The proposed method	0.9517	0.9012	0.8529	0.6998

4.4 Results on the MSTAR Public T-72 Variants Dataset

In another scenario, the proposed method is evaluated on the more challenging T-72 eight-target classification problem, as all the targets are almost indistinguishable. The number and the depression angles of the training and the testing sample images are listed in Table 5. The single and overall accuracies are explained in Tables 6 and 7, respectively. The confusion matrix is presented in Figure 12.

TABLE 5 THE MSTAR PUBLIC T-72 VARIANTS DATASET: THE NUMBER AND THE DEPRESSION ANGLES OF TRAINING AND TESTING SAMPLES USED IN THE EXPERIMENTS.

Target	Train		Test	
	Depression	Number of Images	Depression	Number of Images
A04	17°	299	15°	274
A05	17°	298	15°	274
A07	17°	299	15°	274
A10	17°	296	15°	271
A32	17°	298	15°	274
A62	17°	299	15°	274
A63	17°	299	15°	273
A64	17°	298	15°	274

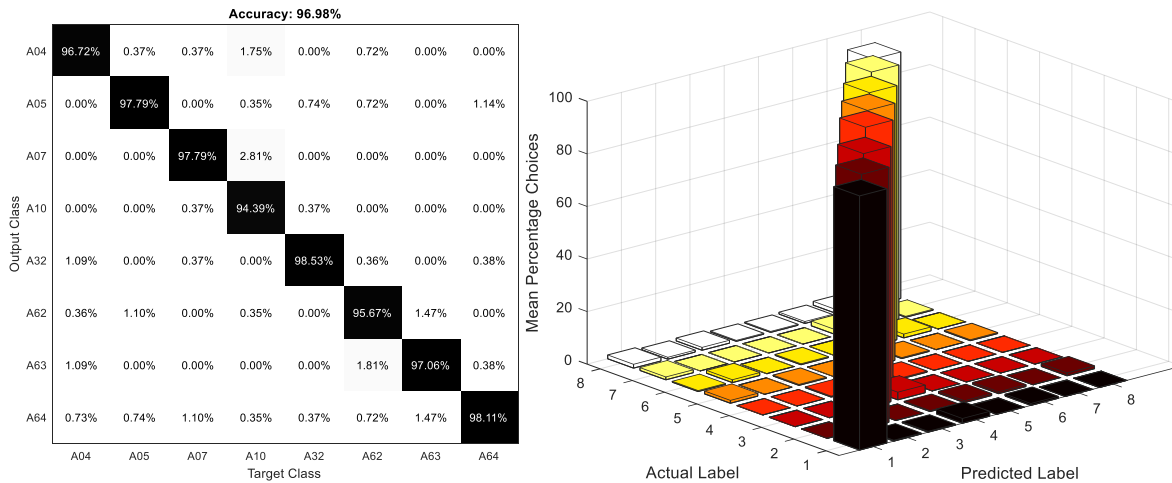


Fig.12. Confusion matrix of the proposed method on T-72 Variants dataset. The rows and columns of the matrix indicate the actual and predicted classes, respectively.

4.5 Results on the MSTAR with Large Depression Angle Variations

Since SAR images are very sensitive to depression angle variation, the credibility of the proposed method is further evaluated on large depression angles. In these experiments, four targets (2S1, BRDM-2, T-72, and ZSU-234) with 30° depression angle are assessed. The types and the number of the considered SAR images are shown in Table 8.

TABLE 8 THE MSTAR PUBLIC DATABASE WITH 30° DEPRESSION ANGLE: THE NUMBER OF TRAINING AND TESTING SAMPLES USED IN THE EXPERIMENTS.

Target	Type	Depression	Number of Images
2S1	B01	30°	288
BRDM-2	E71	30°	287
T-72	A64	30°	288
ZSU-234	D08	30°	288

The single and overall accuracies are presented in Tables 9 and 10, respectively. The confusion matrix is shown in Figure 13.

4.6 Comparison with Different Fusion Methods

In order to study the sensitivity of the feature level fusion on classification on the MSTAR database, we compared the classification accuracy with different fusion strategies (CCA, MCCA), SAR-Oriented GBVS [35] and without feature fusion. As shown in Table 11, our proposed method using MCCA achieves the best performance.

TABLE 2 THE CLASSIFICATION ACCURACY FOR EACH TARGET CLASS ON MSTAR PUBLIC MIXED TARGET DATASET

Class	Single Accuracy	Error Single	Total Accuracy	Error Total	Sensitivity	Specificity	Precision	False Positive Rate
BMP-2	0.99825	0.0017452	0.10223	0	0.99825	1	1	0
BTR-70	1	0	0.10223	0.00017873	1	0.9998	0.99825	0.00019908
T-72	0.98255	0.017452	0.10063	0.00089366	0.98255	0.999	0.9912	0.00099562
BTR-60	0.99778	0.0022173	0.080429	0	0.99778	1	1	0
2S1	1	0	0.10241	0	1	1	1	0
BRDM-2	1	0	0.10223	0	1	1	1	0
D7	1	0	0.10223	0	1	1	1	0
T-62	1	0	0.10241	0	1	1	1	0
ZIL-131	0.99824	0.0017575	0.10152	0.00017873	0.99824	0.9998	0.99824	0.00019897
ZSU-234	0.99295	0.0070547	0.10063	0.0017873	0.99295	0.99801	0.98255	0.0019889

TABLE 3 THE OVERALL CLASSIFICATION ACCURACY MSTAR PUBLIC MIXED TARGET DATASET

Accuracy	Error	Sensitivity	Specificity	Precision	False Positive Rate
0.9970	0.0030	0.9970	0.9997	0.9970	3.3825e-04

TABLE 6 THE CLASSIFICATION ACCURACY FOR EACH TARGET CLASS ON MSTAR PUBLIC T-72 VARIANTS DATASET

Class	Single Accuracy	Error Single	Total Accuracy	Error Total	Sensitivity	Specificity	Precision	False Positive Rate
A04	0.96715	0.032847	0.12112	0.0041133	0.96715	0.9953	0.96715	0.0047022
A05	0.9708	0.029197	0.12157	0.0027422	0.9708	0.99687	0.97794	0.0031348
A07	0.9708	0.029197	0.12157	0.0027422	0.9708	0.99687	0.97794	0.0031348
A10	0.99262	0.0073801	0.12294	0.0073126	0.99262	0.99165	0.94386	0.0083464
A32	0.9781	0.021898	0.12249	0.0018282	0.9781	0.99791	0.98529	0.0020899
A62	0.96715	0.032847	0.12112	0.0054845	0.96715	0.99373	0.95668	0.0062696
A63	0.96703	0.032967	0.12066	0.0036563	0.96703	0.99582	0.97059	0.0041775
A64	0.94526	0.054745	0.11837	0.0022852	0.94526	0.99739	0.98106	0.0026123

TABLE 7 THE OVERALL CLASSIFICATION ACCURACY ON MSTAR PUBLIC T-72 VARIANTS DATASET

Accuracy	Error	Sensitivity	Specificity	Precision	False Positive Rate
0.9698	0.0302	0.9699	0.9957	0.9701	0.0043

TABLE 9 THE CLASSIFICATION ACCURACY FOR EACH TARGET CLASS ON MSTAR PUBLIC DATABASE WITH 30° DEPRESSION ANGLE

Class	Single Accuracy	Error Single	Accuracy in Total	Error in Total	Sensitivity	Specificity	Precision	False Positive Rate
2S1	0.98958	0.010417	0.24761	0.0026064	0.98958	0.99652	0.98958	0.0034762
BRDM-2	0.98955	0.010453	0.24674	0.004344	0.98955	0.99421	0.9827	0.005787
T-72	0.98264	0.017361	0.24587	0.0026064	0.98264	0.99652	0.98951	0.0034762
ZSU-234	0.99306	0.0069444	0.24848	0.0017376	0.99306	0.99768	0.99306	0.0023175

TABLE 10 THE OVERALL CLASSIFICATION ACCURACY ON MSTAR PUBLIC DATABASE WITH 30° DEPRESSION ANGLE

Accuracy	Error	Sensitivity	Specificity	Precision	False Positive Rate
0.9887	0.0113	0.9887	0.9962	0.9887	0.0038

TABLE 11 COMPARISON WITH DIFFERENT FUSION METHODS ON MSTAR DATABASE

Method	MSTAR public mixed target (%)	MSTAR public T-72 Variants (%)	MSTAR with 30° (%)
Proposed without fusion	98.79	94.50	96.13
VDCCA	99.12	95.31	97.55
VDMCCA	99.70	96.98	98.87
SAR-Oriented GBVS [35]	99.68	96.90	98.70

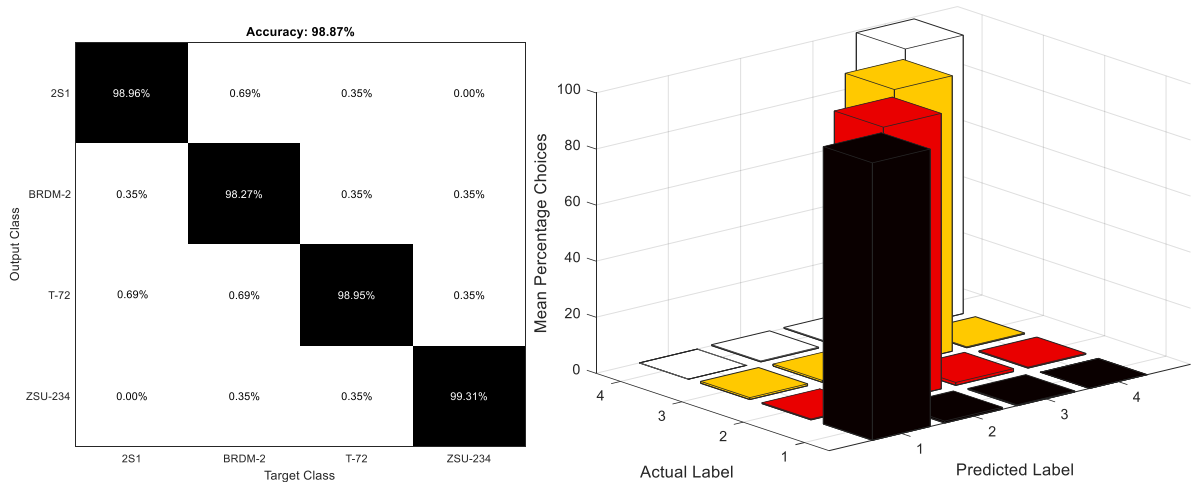


Fig.13. Confusion matrix of the proposed method on MSTAR with large depression angle variations. The rows and columns of the matrix indicate the actual and predicted classes, respectively.

4.7 Influence of Number of Layers and Different Receptive Fields on the Results

To study the effect of network depth on its accuracy in SAR image recognition setting, several successful CNN models pre-trained on MSTAR are evaluated in our work, which are the famous baseline model AlexNet, the Caffe reference model (CaffeRef), and the VGG network [36]. Due to a large learning capacity, dominant expressive power and hierarchical structure of our SAR oriented very deep network (19 layers): a high-level, semantic and robust feature representation for each region proposal is obtained as it is illustrated in Table 12.

TABLE 12 THE EFFECT OF NETWORK DEPTH ON THE PERFORMANCE

Models	Accuracy (%)								MSTAR public mixed	MSTAR T-72 Variants	MSTAR depression 30°
	Conv1	Conv2	Conv3	Conv4	Conv5	Fc1	Fc2	Fc3			
AlexNet	11×11×96	5×5×256	3×3×384	3×3×384	3×3×256	4096 dropout	4096 dropout	C softmax	95.21	86.82	89.66
CaffeRef	11×11×96	5×5×256	3×3×384	3×3×384	3×3×256	4096 dropout	4096 dropout	C softmax	95.45	85.96	88.99
VGGF	11×11×64	5×5×256	3×3×256	3×3×256	3×3×256	4096 dropout	4096 dropout	C softmax	95.66	86.9	90.6
VGGM	7×7×96	5×5×256	3×3×512	3×3×512	3×3×512	4096 dropout	4096 dropout	C softmax	96.7	88.08	91.5
VGGM-128	7×7×96	5×5×256	3×3×512	3×3×512	3×3×512	4096 dropout	128 dropout	C softmax	96.13	89.43	90.12
VGGM-1024	7×7×96	5×5×256	3×3×512	3×3×512	3×3×512	4096 dropout	1024 dropout	C softmax	97.6	90.86	91.6
VGGM-2048	7×7×96	5×5×256	3×3×512	3×3×512	3×3×512	4096 dropout	2048 dropout	C softmax	96.74	90.12	91.55
VGGS	7×7×96	5×5×256	3×3×512	3×3×512	3×3×512	4096 dropout	4096 dropout	C softmax	97.95	91.66	92.88
VGG16	16 weight layers including 13 convolutional layers 3×3 and 3 fully-connected layers								99.1	95.39	97.1
SAR-OVDN (19 weight layers including 16 convolutional layers and 3 fully-connected layers)									99.7	96.98	98.87

In addition, using a stack of two 3×3 convolutional layers (without pooling in between) has a 5×5 effective receptive field, and using three of 3×3 layers has a 7×7 effective receptive field. So the reasons for using, for instance, a stack of three 3×3 convolutional layers instead of a single 7×7 layer are: First, we integrate three non-linear rectification layers rather than one, which leads to a more discriminative decision function. Second, we reduce the number of parameters by supposing that the three layer 3×3 convolution stack has K channels, and the stack is parameterized by $3(3^2K^2) = 27K^2$ weights; in contrast to a single 7×7 convolutional layer which requires $7^2K^2 = 49K^2$, which needs **81%** more of parameters.

4.8 Comparison with Recent Representative Methods

The classification performance of the proposed method is compared with the most widely cited approaches and the recent representative paradigms such as: MSRC [34], SVM [37], Cond Gauss [38], MSS [39], A-Convnets [4], CNN [5], BCS [40], CNN-SVM [15] and Deep Learning [16]. Because the SVM method [37] only considers the three-target classification problem, we have run the published online code from [37] to obtain the results on our classification tasks (ten targets, T-72 Variants, and 30° depression angle). All other compared methods do the same classification tasks as ours. Therefore, we directly use the classification accuracies presented in the corresponding papers. As illustrated in Table 12, our proposed method achieves the highest accuracy rates. Fig. 14 shows MSTAR/IU Mixed Targets recognition results based on MF datasets.



Fig. 14. MSTAR/IU Mixed Targets recognition results using different MF datasets

TABLE 13

THE PERFORMANCE COMPARISON BETWEEN THE PROPOSED METHOD AND THE STATE-OF-THE-ART METHODS ON THE MSTAR PUBLIC DATABASE

Method	MSTAR public mixed target (%)	MSTAR public T-72 Variants (%)	MSTAR with 30° (%)
SVM [37]	90	78.5	81
Cond Gauss [38]	97	77.32	80
MSRC [34]	93.6	-	98.4
MSS [39]	96.6	-	98.2
CNN [5]	84.7	81.08	81.56
A-Convnets [4]	99.13	95.43	96.12
BCS [40]	92.6	88.76	92.6
Deep Learning [16]	92.74	-	-
CNN-SVM [15]	99.5	95.75	96.6
Proposed with softmax	99.51	96.13	98.34
Proposed with SVM	99.70	96.98	98.87

5 Conclusion

This paper developed SAR Oriented network to automatically learn very deep features from the data sets, selects adaptive feature layers, and fuses the learned features. The proposed network increases the depth by using more convolutional layers to lessen the speckle noise effect. A dropout technique is supplied to deal with the over-fitting problem due to limited training data sets. In addition, the MCCA algorithm is introduced to combine the selective adaptive layer's features and improves the representations with respect to the correlation objective measured on SAR target images, making the proposed method feasible for SAR image processing. Experimental results on the benchmark of MSTAR database demonstrate the effectiveness of the proposed method compared with the state-of-the-art methods.

References

1. C. F. Olson and D. P. Huttenlocher, "Automatic target recognition by matching oriented edge pixels," *IEEE Transactions on image processing*, vol. 6, no. 1, pp. 103–113, 1997.
2. M. Amrani, S. Chaib, I. Omara, and F. Jiang, "Bag-of-visual-words based feature extraction for sar target classification," in *Ninth International Conference on Digital Image Processing (ICDIP 2017)*, vol. 10420. International Society for Optics and Photonics, 2017, p. 104201J.
3. Amrani, M., Yang, K., Zhao, D., Fan, X., & Jiang, F. (2017, September). An efficient feature selection for SAR target classification. In *Pacific Rim Conference on Multimedia* (pp. 68-78). Springer, Cham.

4. S. Chen, H. Wang, F. Xu, and Y.-Q. Jin, "Target classification using the deep convolutional networks for sar images," *IEEE Transactions on Geoscience and Remote Sensing*, vol. 54, no. 8, pp. 4806–4817, 2016.
5. N. Srivastava, G. E. Hinton, A. Krizhevsky, I. Sutskever, and R. Salakhutdinov, "Dropout: a simple way to prevent neural networks from overfitting." *Journal of machine learning research*, vol. 15, no. 1, pp. 1929–1958, 2014.
6. H. Furukawa, "Deep learning for target classification from sar imagery: Data augmentation and translation invariance," *arXiv preprint arXiv:1708.07920*, 2017.
7. S. Chen and H. Wang, "Sar target recognition based on deep learning," in *Data Science and Advanced Analytics (DSAA), 2014 International Conference on*. IEEE, 2014, pp. 541–547
8. K. Du, Y. Deng, R. Wang, T. Zhao, and N. Li, "Sar atr based on displacement-and rotation-insensitive cnn," *Remote Sensing Letters*, vol. 7, no. 9, pp. 895–904, 2016.
9. M. Amrani and F. Jiang, "Deep feature extraction and combination for synthetic aperture radar target classification," *Journal of Applied Remote Sensing*, vol. 11, no. 4, p. 042616, 2017.
10. D. C. Ciresan, U. Meier, J. Masci, L. Maria Gambardella, and J. Schmidhuber, "Flexible, high performance convolutional neural networks for image classification," in *IJCAI Proceedings-International Joint Conference on Artificial Intelligence*, vol. 22, no. 1. Barcelona, Spain, 2011, p. 1237.
11. I. J. Goodfellow, Y. Bulatov, J. Ibarz, S. Arnaud, and V. Shet, "Multi-digit number recognition from street view imagery using deep convolutional neural networks," *arXiv preprint arXiv:1312.6082*, 2013.
12. C. Szegedy, W. Liu, Y. Jia, P. Sermanet, S. Reed, D. Anguelov, D. Erhan, V. Vanhoucke, and A. Rabinovich, "Going deeper with convolutions, corr abs/1409.4842," *URL <http://arxiv.org/abs/1409.4842>*, 2014.
13. K. Simonyan and A. Zisserman, "Very deep convolutional networks for large-scale image recognition," *arXiv preprint arXiv:1409.1556*, 2014.
14. C. P. Schwegmann, W. Kleynhans, B. P. Salmon, L. W. Mdakane, and R. G. Meyer, "Very deep learning for ship discrimination in synthetic aperture radar imagery," in *Geoscience and Remote Sensing Symposium (IGARSS), 2016 IEEE International*. IEEE, 2016, pp. 104–107.
15. A. Bochkovskiy, C. Y. Wang, and H. Liao, "YOLOv4: Optimal speed and accuracy of object detection," *arXiv preprint arXiv:2004.10934*, 2020.
16. S. A. Wagner, "Sar atr by a combination of convolutional neural network and support vector machines," *IEEE Transactions on Aerospace and Electronic Systems*, vol. 52, no. 6, pp. 2861–2872, 2016.
17. F. Zhou, L. Wang, X. Bai, and Y. Hui, "SAR ATR of ground vehicles based on LM-BN-CNN", *IEEE Transactions on Geoscience and Remote Sensing*, 2018.
18. E. Mason, B. Yonel, and B. Yazici, "Deep learning for radar," in *Radar Conference (RadarConf), 2017 IEEE*. IEEE, 2017, pp. 1703–1708.
19. Y. LeCun, K. Kavukcuoglu, and C. Farabet, "Convolutional networks and applications in vision," in *Circuits and Systems (ISCAS), Proceedings of 2010 IEEE International Symposium on*. IEEE, 2010, pp. 253–256.
20. Y. Tang, "Deep learning using linear support vector machines," *arXiv preprint arXiv:1306.0239*, 2013.

21. C. Liu and H. Wechsler, "A shape-and texture-based enhanced fisher classifier for face recognition," *IEEE transactions on image processing*, vol. 10, no. 4, pp. 598–608, 2001.
22. J. Yang and J.-y. Yang, "Generalized k-l transform based combined feature extraction," *Pattern Recognition*, vol. 35, no. 1, pp. 295–297, 2002.
23. C. Oliver and S. Quegan, *Understanding synthetic aperture radar images*. SciTech Publishing, 2004.
24. X. Huang, B. Zhang, H. Qiao, and X. Nie, "Local discriminant canonical correlation analysis for supervised polsar image classification," *IEEE Geoscience and Remote Sensing Letters*, vol. 14, no. 11, pp. 2102–2106, 2017.
25. M. J. Canty, *Image analysis, classification and change detection in remote sensing: with algorithms for ENVI/IDL and Python*. Crc Press, 2014.
26. G. Andrew, R. Arora, J. Bilmes, and K. Livescu, "Deep canonical correlation analysis," in *International Conference on Machine Learning*, 2013, pp. 1247–1255.
27. W. Krzanowski, *Principles of multivariate analysis*. OUP Oxford, 2000.
28. J. Ding, B. Chen, H. Liu, and M. Huang, "Convolutional neural network with data augmentation for sar target recognition," *IEEE Geoscience and Remote Sensing Letters*, vol. 13, no. 3, pp. 364–368, 2016.
29. SDMS, "Mstar data," <https://www.sdms.afrl.af.mil/index.php?collection=mstar>, last accessed: 2016-11-23.
30. El-Darymli, K., Mcguire, P., Gill, E. W., Power, D., & Moloney, C. (2015). Characterization and statistical modeling of phase in single-channel synthetic aperture radar imagery. *IEEE Transactions on Aerospace and Electronic Systems*, 51(3), 2071-2092.
31. Olivier, C., & Quegan, S. (1998). *Understanding Synthetic Aperture Radar Images*, Artech House.
32. Vidal-Pantaleoni, A., & Marti, D. (2004). Comparison of different speckle-reduction techniques in SAR images using wavelet transform. *International Journal of Remote Sensing*, 25(22), 4915-4932.
33. Choi, H., Yu, S., & Jeong, J. (2019, June). Speckle Noise Removal Technique in SAR Images using SRAD and Weighted Least Squares Filter. In *2019 IEEE 28th International Symposium on Industrial Electronics (ISIE)* (pp. 1441-1446). IEEE.
34. G. Dong, N. Wang, and G. Kuang, "Sparse representation of monogenic signal: With application to target recognition in sar images," *IEEE Signal Processing Letters*, vol. 21, no. 8, pp. 952–956, 2014.
35. Amrani, M., Jiang, F., Xu, Y., Liu, S., & Zhang, S. (2018). SAR-oriented visual saliency model and directed acyclic graph support vector metric based target classification. *IEEE Journal of Selected Topics in Applied Earth Observations and Remote Sensing*, 11(10), 3794-3810.
36. Zhou, W., Newsam, S., Li, C., & Shao, Z. (2017). Learning low dimensional convolutional neural networks for high-resolution remote sensing image retrieval. *Remote Sensing*, 9(5), 489.
37. U. Srinivas, V. Monga, and R. G. Raj, "Sar automatic target recognition using discriminative graphical models," *IEEE transactions on aerospace and electronic systems*, vol. 50, no. 1, pp. 591–606, 2014.
38. J. A. O'Sullivan, M. D. DeVore, V. Kedia, and M. I. Miller, "Sar atr performance using a conditionally gaussian model," *IEEE Transactions on Aerospace and Electronic Systems*, vol. 37, no. 1, pp. 91–108, 2001.

39. G. Dong and G. Kuang, "Classification on the monogenic scale space: application to target recognition in sar image," *IEEE Transactions on Image Processing*, vol. 24, no. 8, pp. 2527–2539, 2015.
40. X. Zhang, J. Qin, and G. Li, "Sar target classification using bayesian compressive sensing with scattering centers features," *Progress In Electromagnetics Research*, vol. 136, pp. 385–407, 2013.